Effective surface viscosities of a particle-laden fluid interface

S. V. Lishchuk and I. Halliday
Materials and Engineering Research Institute, Sheffield Hallam University, Howard Street, Sheffield S1 1WB, United Kingdom
(Received 16 October 2008; revised manuscript received 10 June 2009; published 10 July 2009)

The Einstein formula for the effective shear viscosity of low Reynolds number suspension flows is generalized to the case of flat, low-concentration, particle-laden interfaces separating two immiscible fluids. The effective surface shear and dilational viscosities of this system is found to be $\eta_s=\frac{5}{3}(\eta_1+\eta_2)R\phi$ and $\zeta_s=5(\eta_1+\eta_2)R\phi$, correspondingly, where η_1 and η_2 are the shear viscosities of two bulk fluids and ϕ is the surface concentration of spherical particles of radius R. The formula is found to be in excellent agreement with data obtained using multicomponent lattice Boltzmann equation simulation.

DOI: 10.1103/PhysRevE.80.016306 PACS number(s): 47.55.Kf, 47.55.N−, 47.11.−j

I. INTRODUCTION

To minimize total interfacial energy, suspended particles can self-assemble on the surface of a droplet of one liquid suspended in a second, immiscible, liquid [1]. In fact, this process was observed by Ramsden [2] as long ago as 1903. Rather more recently, rekindled interest in the same, essential, phenomenon has focused on the important use of liquid-liquid interfaces as templates for the self-assembly of microparticles [3] and, still more recently, for nanoparticles [4,5]. Consequently, the properties of colloidal particles at liquid-liquid interfaces have attracted significant recent attention.

In fact, systems similar to those identified above have wide-ranging current applications, which we proceed selectively (and briefly) to highlight, now. Surfactant-free *Pickering* emulsions, stabilized by solid particles, are routinely encountered in recovery, separation, and cleaning of oil, cosmetic preparation, and waste water treatment. Recently added to this list are new applications with environmental implications [6] and new commercial applications, from remediation [7], through the production of porous media [8], to paints with new optical properties [9]. Further afield, droplets with micron-scale, particle-laden interfaces serve as prototype vesicles, or colloidosomes, and facilitate the study of interparticle interactions at interfaces (but are probably more important as prototype selectively permeable membranes which transport submicron particles into the colloidosome, but exclude micron-sized particles [10]). Still further afield, advances have been made in the use of self-assembled submicrometer colloidal particles at liquid-liquid interfaces to investigate mesoscale structure formation and two-dimensional melting. All the systems mentioned above share in common the fact that the particle-laden interfaces which comprise them are central to any understanding.

The dynamic properties of particle-laden interfaces are strongly influenced by direct interparticle forces (capillary, steric, electrostatic, van der Waals, etc.) and complicated hydrodynamic interactions mediated by the surrounding fluid [11–14]. At macroscopic scales, the rheological properties of the particle-laden fluid interface can be viewed as those of a liquid-liquid interface with some *effective* surface viscoelastic properties described by effective surface shear and compressional viscoelastic moduli.

In fact, a particle-laden interface may be viewed as a quasi-two-dimensional colloid. The effective shear viscosity of a three-dimensional suspension of solid particles can be calculated when the concentration of particles is low, so that interactions of particles can be neglected. The resulting effective shear viscosity η_{eff} for this case was calculated by Einstein [15] back in 1906 in the low Reynolds number (Stokes' regime) limit and is given by the Einstein formula

$$\eta_{\text{eff}}=\eta\left(1+\frac{5}{2}\phi_V\right), \tag{1}$$

where η is the shear viscosity of the bulk fluid and ϕ_V is the total volume fraction occupied by the particles. This formula describes experimental data at low concentrations very well, and, further, can be used as a starting approximation for more complicated systems in which the interparticle interactions of a different nature cannot be any longer neglected. Importantly, such a constitutive relation as that given in Eq. (1) can be used to simplify numerical calculations by allowing one to avoid explicit modeling of the flow-advected species.

Following Einstein, this paper aims to obtain expressions for the effective surface viscosities of a fluid interface laden with micron-scale particles at low surface concentration. The main restriction in our analysis arises from the fact that particles at the interface between two different fluids can, in general, take any contact angles. We optimize symmetry and assume a particle-liquids contact angle of $\pi/2$ rad. Calculation of the mobility of the widely separated particles at the surface of a fluid presents a complicated problem [12] but considerable simplification can be achieved in this special case when surface tensions in the system are large and give a contact angle of $\pi/2$. Then, the particles will embed symmetrically in each of the separated fluid phases and the problem acquires additional symmetry so that derivation of effective interfacial properties can be pursued precisely along lines of the calculation of Einstein.

First, in Sec. II, we present background details. In Sec. III we derive an analog of the Einstein's formula for the effective surface viscosities of low-concentration particle-laden interfaces with large interfacial tension between two immiscible fluids, then, in Sec. IV, test the validity of our result and consider larger concentrations (by using lattice Boltzmann simulations). We present our conclusions in Sec. V. Details

of the simulation method and an analysis of the stability of the system studied are presented in the two appendixes.

II. BACKGROUND

It is important to set the present work within the context of two particular previous calculations, also performed in the zero Reynolds number approximation. First, in Ref. [16], Tambe and Sharma consider a fluid-fluid interface with structure. They take an interface to consist of a thin but three-dimensional interfacial fluid slab immersed in which is a monodisperse population of spherical particles that can impress forces on each other (giving viscoelastic properties to the effective interface). The calculations of Tambe and Sharma invoke properties of three-dimensional, symmetric, bulk suspensions to determine the hydrodynamic contribution to a general interfacial stress, which contains additional, elastic, interparticle contributions, recall, to predict an effective interfacial viscosity over a range of surface coverage up to about 70%.

Second, in Ref. [17], Henle and Levine consider transport in cellular membranes using as a model a two-dimensional membrane fluid decorated by a small population of flat 2D disks each of radius a. After the manner of Einstein, these workers obtain an expression for the effective surface shear viscosity, η_M, as a function of the two-dimensional membrane fluid's viscosity, the surface volume fraction of disks and the parameter:

$$\epsilon = a/l_0, \quad l_0 \equiv \eta_M/\eta, \tag{2}$$

where l_0 is the *Saffman-Delbrück* length scale [18]. In the last equation, η is the bulk three-dimensional fluid's shear viscosity. Henle and Levine [17] achieve a description that exposes the role of the Saffman-Delbrück length scale.

In contrast to the above two works, we give in the next section a rather more direct derivation, after Einstein [15], but here for the surface shear and dilational viscosities of a flat interface populated by symmetrically embedded, fully three-dimensional, monodisperse, micron-scale, spherical particles assumed to have a diameter that is very large relative to the interface cross section (which we consider to be *molecular*). Put another way, our assumptions in respect of length scales permit us to neglect all fluid-fluid interface structures. This assumption is completely consistent with an analysis aimed at the continuum regime. It means, however, that all the calculations presented in the next section must be taken to apply in the limit of large $\epsilon = a/l_0$. In support of this assumption, we note that, for typical liquids, without the presence of any surfactant, the length l_0 is indeed very small compared with a micron-scale particle. Our analysis further contrasts with previous works in that it accounts for a shear viscosity contrast between the separated bulk liquids and it also contains only directly measurable parameters of separated fluids' shear viscosities and particles' radius.

We shall neglect the effects of contact line slip in our analysis and, again, suppose the discontinuous continuum interface to have no structure whatsoever. We shall further assume a large interfacial tension. The need for the latter assumption is explained in Appendix A.

III. SURFACE VISCOSITIES AT LOW CONCENTRATIONS

In this section we obtain, in a compact analysis, by a direct and transparent generalization of Batchelor's analysis of suspensions [19] both the surface shear and the surface dilatational viscosity. We consider the steady state of a flow of a system of solid spherical particles of radius R, trapped at the flat interface between two incompressible fluids, designated 1 and 2, with densities ρ_I and shear viscosities η_I, $I = 1, 2$. We shall assume that the interfacial tensions favor a contact angle $\pi/2$, so that, in equilibrium, the fluid interface is planar and the centers of particles are located in the interfacial plane.

Consider a volume, V, occupied by two incompressible fluids, each of equal volume, $V/2$, divided by a flat interface of area A, supposed to lie in the x-y plane. We define the surface concentration of particles as

$$\phi = \frac{\pi R^2 N}{A}, \tag{3}$$

with N being the number of particles in area A.

We shall consider the shear flow in the system with the motion of the fluid when unperturbed by particles being described by the velocity field

$$v_i^{(0)} = \alpha_{ij} x_j, \tag{4}$$

where the rate-of-strain tensor, α_{ij}, is symmetric, traceless, and constant. The applied rate of strain, α_{ij}, is supposed to be small and the unperturbed pressure is taken to be zero. The particle-laden interface is supposed always to be flat (see Appendix A).

It is well known that a shear flow distribution may be decomposed into a symmetric shear (which, on general grounds of symmetry, exerts no torque) and a rotation. By considering the motion in an appropriately chosen uniformly rotating rest frame, we need concern ourselves solely with the dissipation associated with a symmetric shear. Further, to ensure that the velocity is parallel to the interfacial plane XY, the symmetric rate-of-strain tensor has to have the form

$$\alpha = \begin{pmatrix} S_{xx} & S_{xy} & 0 \\ S_{yx} & S_{yy} & 0 \\ 0 & 0 & \alpha_{zz} \end{pmatrix}, \tag{5}$$

where

$$S_{ij} = \frac{1}{2}\left(\frac{\partial v_j}{\partial x_i} + \frac{\partial v_i}{\partial x_j}\right) \tag{6}$$

is 2×2 surface rate-of-strain tensor, and $\alpha_{zz} = -S_{xx} - S_{yy}$, to ensure the incompressibility of the fluids.

To find an expression for the effective surface shear viscosity of the particle-laden interface as a whole, we shall compare expressions for the rate of viscous dissipation calculated in two cases. We shall shortly consider a particle-laden interface explicitly. First let us approximate the system as having an effective continuum interface with effective dilational and shear viscosities ζ_s and η_s, respectively.

Consider a sphere of radius r_0 exactly divided into two hemispheres of equal volume by the interface. The area of

the interface contained within this control volume is

$$A = \pi r_0^2. \tag{7}$$

In the case of an effective continuum interface, the rate of viscous dissipation in the bulk liquids contained within our control volume is obtained by an appropriate volume integration [20],

$$\dot{E}^{(0)}_{\text{bulk}} = -\frac{\eta_1}{2}\int_{z>0,r<r_0}\left(\frac{\partial v_i^{(0)}}{\partial x_j}+\frac{\partial v_j^{(0)}}{\partial x_i}\right)^2 dV - \frac{\eta_2}{2}\int_{z<0,r<r_0}\left(\frac{\partial v_i^{(0)}}{\partial x_j}+\frac{\partial v_j^{(0)}}{\partial x_i}\right)^2 dV, \tag{8}$$

in which dV denotes the volume element. With the (shear) velocity distribution identified in Eq. (4), Eq. (8) predicts, for the effective continuum system, the following dissipation rate:

$$\dot{E}^{(0)}_{\text{bulk}} = -\frac{2}{3}\pi r_0^3(\eta_1+\eta_2)\alpha_{ij}\alpha_{ij}. \tag{9}$$

Additionally, of course, there is dissipation due to surface flow given by

$$\dot{E}_{\text{surf}} = -\frac{1}{2}\int_A \sigma'^{(s)}_{ij}\left(\frac{\partial v_i}{\partial x_j}+\frac{\partial v_j}{\partial x_i}\right)dA, \tag{10}$$

where $\sigma^{(s)}_{ij}$ is the surface viscous stress tensor, which has the form [21]

$$\sigma'^{(s)}_{ij} = \zeta_s S_{kk}\delta_{ij} + \eta_s E_{ijkl}S_{kl}, \tag{11}$$

with

$$E_{ijkl} = \delta_{ik}\delta_{jl} + \delta_{il}\delta_{jk} - \delta_{ij}\delta_{kl}, \tag{12}$$

where, again, ζ_s is the dilational (compressional) viscosity and η_s is the surface shear viscosity. For the flow given by Eq. (4) with rate of strain (5), the rate of viscous dissipation Eq. (10) takes the form

$$\dot{E}_{\text{surf}} = -A[2\eta_s S_{ij}S_{ij} + (\zeta_s - \eta_s)(S_{kk})^2]. \tag{13}$$

Next we proceed to obtain our second expression for the rate of viscous dissipation. Consider a single particle, located at the origin (see Fig. 1) in a very thin (i.e., unstructured), flat, sheared interface. Then, due to the symmetry of the problem and the kinematic condition of impenetrability, the velocity field in both the separated fluids is the same and identical to that of associated with the same particle suspended in a single homogeneous fluid. This velocity field is, note, independent of the fluids' shear viscosities: it is the well-known Stokes' regime result [20] adapted for the unperturbed flow in Eq. (4):

$$v_i = v_i^{(0)} + \frac{5}{2}\left(\frac{R^5}{r^4}-\frac{R^3}{r^2}\right)\alpha_{ij}n_i n_j n_k - \frac{R^5}{r^4}\alpha_{ij}n_j, \tag{14}$$

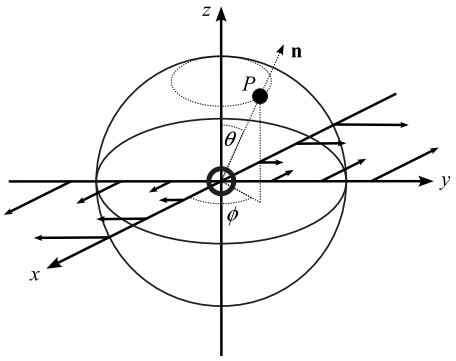

FIG. 1. A solid spherical particle (indicated by the solid line) embedded in the fluid-fluid interface, which lies in the $z=0$ plane. The origin of coordinates, O, is taken to lie at the center of the spherical particle. Elements of our Cartesian and spherical-polar coordinate systems are shown. In particular, the z axis of the Cartesian system coincides with the normal to the fluid-fluid interface. For $z>0(z<0)$ fluid is taken to have shear viscosity $\eta_1(\eta_2)$. Fluid velocity vectors corresponding to a symmetric shear flow (our assumed unperturbed flow) are drawn in the plane $z=0$ (only).

$$p^{(1)} = -5\eta_1\frac{R^3}{r^3}\alpha_{ij}n_i n_j, \quad p^{(2)} = -5\eta_2\frac{R^3}{r^3}\alpha_{ij}n_i n_j, \tag{15}$$

in which r is the radial coordinate and $\mathbf{n}$ is the unit radial vector (see Fig. 1) over the particle surface. In the last equation, $p^{(1)}(p^{(2)})$ is the pressure within fluid 1 (2). We reserve further discussion of this solution and, in particular, the pressure field to Appendix A.

We now proceed to determine the dissipation rate when particles are explicitly accounted for. Following Batchelor [19], we exploit the symmetry of the problem in the rest frame of a single particle (see above) and consider dissipation inside the finite spherical region which is bisected by the interface, $z=0$, to form a pair of hemispherical regions $z<0$, $z>0$ (see Fig. 1). The upper (lower) hemispherical surface of this region is embedded in the fluid with shear viscosity $\eta_1(\eta_2)$ and is denoted by $a_1(a_2)$. The full spherical surface, which is denoted by A_1, contains a volume V. Recalling that the unperturbed pressure has been taken to be zero, the rate at which forces do work on this *external* boundary is obtained from the expression [19]

$$\alpha_{ik}\int_{a_1}(\sigma^{(1)}_{ij}+2\eta_1\alpha_{ij})x_k n_j dA + \alpha_{ik}\int_{a_2}(\sigma^{(2)}_{ij}+2\eta_2\alpha_{ij})x_k n_j dA. \tag{16}$$

In the last equation, the excess strain rate,

$$S'_{ij} = \frac{1}{2}\left[\frac{\partial}{\partial x_i}(v_j - v_j^{(0)}) + \frac{\partial}{\partial x_j}(v_i - v_i^{(0)})\right], \tag{17}$$

defines the excess stresses of each of the two fluids:

$$\sigma^{(I)}_{ij} = -p^{(I)}\delta_{ij} + 2\eta_n S_{ij}, \quad I = 1,2. \tag{18}$$

Note, for a homogeneous system, with no surface effects, the expression in Eq. (16) would evaluate to

$$\alpha_{ij}\alpha_{ij}\left[2\eta_1\left(\frac{V}{2}\right)+2\eta_2\left(\frac{V}{2}\right)\right]. \tag{19}$$

Viscous dissipation within the fluid bounded, externally, by A_1 and, internally, by the particle surface, is assumed to account for the work identified in expression Eq. (16). Further, Batchelor's use of the divergence theorem [19] is not obstructed by the albeit discontinuous change in the value of shear viscosity on the external boundary A_1 and within the volume V, so the gradient terms (in S'_{ij}) in expression of Eq. (16) may be transformed to surface contributions from the *internal* particle surface, together with a volume integral of "divergence" $\partial_j(\sigma^{(l)}_{ij}x_k)$, which vanishes in the steady Stokes flow regime (since $\partial\sigma_{ij}/\partial x_j=0$). The expression in equation Eq. (16) then becomes

$$-2R\eta_1\alpha_{ik}\alpha_{ij}\int_{s_1} n_j n_k dA - 2R\eta_2\alpha_{ik}\alpha_{ij}\int_{s_2} n_j n_k dA + \alpha_{ik}\int_{s_1}\sigma^{(1)}_{ij}x_k n_j dA + \alpha_{ik}\int_{s_2}\sigma^{(2)}_{ij}x_k n_j dA, \tag{20}$$

where $s_1(s_2)$ denotes the upper (lower), internal surface of the particle (radius R, recall) and n_k the k component of the unit surface normal, i.e., the k component of the unit radial vector. Note that contributions from surface integrals of stress over the flat volume-bisecting interface, A, do not appear in Eq. (20) for such contributions cancel, because of the boundary conditions on stress at a plane interface. With the help of Eqs. (14) and (15) and the fact that

$$R\int_{s_1} n_j n_k dA = \frac{2\pi R^3}{4}\delta_{ij}, \tag{21}$$

(as is straightforwardly verified) the viscous dissipation in the particle system, $\dot{E}_{\text{part}}$, may now be calculated from well-behaved surface integrals performed over internal particle surfaces s_1 and s_2, using Eqs. (14), (15), and (18). Finally, supposing N particles all to be mutually separated by distances large compared with R, the disturbance flow $(v_i-v_i^{(0)})$ due to one particle will be small close to any other, we obtain

$$\dot{E}_{\text{part}} = -\frac{10\pi}{3}(\eta_1+\eta_2)R^3\alpha_{ik}\alpha_{ik}N, \tag{22}$$

which, using Eq. (3) can be written as

$$\dot{E}_{\text{part}} = -\frac{10}{3}(\eta_1+\eta_2)R\alpha_{ik}\alpha_{ik}A\phi. \tag{23}$$

Substituting, according to Eq. (5), $\alpha_{ik}\alpha_{ik}=S_{ik}S_{ik}+(S_{kk})^2$, we finally obtain

$$\dot{E}_{\text{part}} = -\frac{10}{3}(\eta_1+\eta_2)R[S_{ik}S_{ik}+(S_{kk})^2]A\phi. \tag{24}$$

Supposing that the additional dissipation expressed above is attributable to the effects of the interfacial particles, and therefore equating the right-hand sides of Eqs. (13) and (24), we finally obtain for the effective viscosities of a discontinuous interface between fluids of shear viscosity η_1 and η_2 decorated with spherical particles of radius R:

$$\eta_s = \frac{5}{3}(\eta_1+\eta_2)R\phi \tag{25}$$

and

$$\zeta_s = 5(\eta_1+\eta_2)R\phi. \tag{26}$$

Wilson and Davis [22] have, using different methods, derived results that agree with Eq. (25). A critical point to note in respect of our own analysis is that it has been possible, in the above manner, to derive the dilational surface viscosity, by considering an appropriate shear flow of bulk incompressible fluid. This is comparable to the situation when, in three dimensions, one considers a compressible flow to obtain the expression for the effective bulk viscosity of suspensions [23]. Further support for our analytical results of this section may be obtained from computer simulations, which we now proceed to consider.

IV. SURFACE SHEAR VISCOSITY AT HIGHER CONCENTRATIONS

In this section we calculate effective surface shear viscosity of a particle-laden fluid interface at larger concentration of particles and so extend our investigation to larger concentrations. In order to do this we employ the modification of the lattice Boltzmann method [24] used previously to calculate the suspension viscosity by the direct calculation of dissipation in simulations bounded by modified Lees-Edwards (LE) periodic boundary conditions [25].

Consider a three-dimensional volume $V=A\times L_z=L_x\times L_y\times L_z$ filled with incompressible fluid. N spherical particles are immersed into the fluid and their centers are confined in the X-Y plane ($z=0$). This corresponds to the special case of the original system in which both fluids have the same density and viscosity, and the surface tension is strong enough to prohibit motion of particles perpendicular to the interface. In the present context, although the particles are confined to the interfacial plane, their surface boundary conditions (which correspond to no-slip) in no way prevent their free rotation.

Periodic boundary conditions are applied in three directions. Constant shear in X-Y plane is imposed by using Lees-Edwards boundary conditions [26,27] in Y direction, which provides the constant difference v_{LE} in v_x component of velocity between planes $y=0$ and $y=L_y$. The details of the lattice Boltzmann algorithm used in the present paper are given in Appendix B.

After the procedure in Sec. III, we write the energy dissipation in the volume V as

$$\dot{E} = -\frac{\eta}{2}\int_V\left(\frac{\partial v_j}{\partial x_i}+\frac{\partial v_i}{\partial x_j}\right)^2 dV \tag{27}$$

$$-\frac{\eta_s}{2}\int_A\left(\frac{\partial v_j}{\partial x_i}+\frac{\partial v_i}{\partial x_j}\right)^2 dA, \tag{28}$$

and using

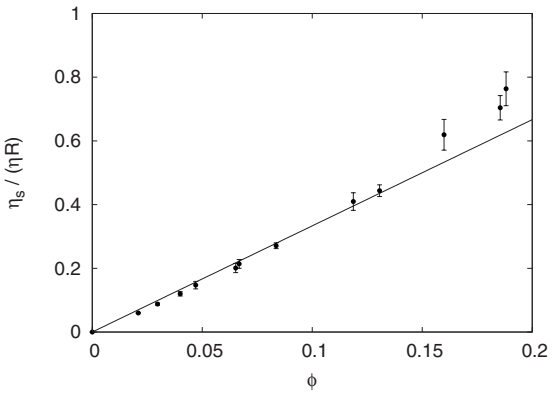

FIG. 2. Dependence of surface shear viscosity upon surface concentration. Points are calculated by LB simulation; line corresponds to Eq. (25).

$$\frac{\partial v_j}{\partial x_i} + \frac{\partial v_i}{\partial x_j} = 2\alpha_{ij} \tag{29}$$

we obtain straightforwardly the formula for simulation data analysis,

$$\frac{1}{2}\dot{E} = (V\eta + A\eta_s)\alpha_{ij}^2, \tag{30}$$

or, on observing $\alpha_{ij}^2 = (v_{LE}/L_y)^2$,

$$\frac{1}{2}\dot{E} = (V\eta + A\eta_s)\frac{v_{LE}^2}{L_y^2}. \tag{31}$$

Once $\dot{E}$ has been measured [25] within a chosen volume, V, and interfacial region, A, for a chosen lattice fluid shear viscosity, η, (see Appendix B), v_{LE} and L_y, Eq. (31) may be used directly to evaluate an effective surface viscosity, η_s.

Figure 2 presents the effective shear viscosity obtained for different sizes and concentrations of particles compared with Eq. (25). The agreement is satisfactory for

$$\phi \leq 0.15. \tag{32}$$

Inequality (32) gives the region of applicability of low-concentration formula (25). Our results are, again, in agreement with those of Wilson and Davis [22].

V. CONCLUSION

In the main result of this paper, we have obtained, from a calculation performed in the continuum approximation of large $\epsilon = a/l_0$ (where l_0 is the Saffman-Delbrück length [see Eq. (2)]), a simple expression for the steady effective surface shear viscosity of a two-dimensional colloid system comprised of widely separated spherical particles at the interface between two immiscible liquids, for the special case of a solid-fluid contact angle (between particles' surface and fluid-fluid interface) of $\pi/2$ rad. The result, given by Eq. (25), is demonstrated to give satisfactory agreement with multicomponent lattice Boltzmann equation method simulations for concentration of particles up to ~0.15. While the experiments of Cicuta *et al.* [28], reporting data on elastic, G', and viscous, G'', interfacial shear moduli and concerning much larger particle concentrations, do not resolve the regime of our calculation in sufficient detail to make comparison possible, it can be claimed that these data are, very broadly, in agreement with ours.

The result, Eq. (25), can be used directly for low-concentration systems or as a starting point for several extensions. These may include particle-laden fluid interfaces with arbitrary contact angles, larger concentrations of particles, nonhydrodynamic interactions between particles, anisotropic particles (e.g., ellipsoids, rods), anisotropic fluids (e.g., nematic liquid crystals), polydisperse particles, higher shear rates, and time-dependent flows (shear viscoelastic modulus). We hope that this work is a step toward the solution of the problem of characterization of effective viscoelastic properties of particle-laden fluid interfaces basing on the properties of constituent particles and fluids.

APPENDIX A: CONFIGURATIONAL STABILITY

Figure 1 shows a single solid spherical particle embedded in the fluid-fluid interface, which is taken to lie in the $z=0$ plane. The origin of coordinates, O, is taken to lie at the center of the sphere. Elements of Cartesian and spherical polar coordinate systems are shown. In particular, the z axis of the Cartesian system coincides with the normal to the fluid-fluid interface. For $z>0 (z<0)$, fluid is taken to have shear viscosity $\eta_1(\eta_2)$. The shear flow, indicated by solid arrows, lies in the plane of the interface, $z=0$. For any point, P, on the spherical particle surface, the surface normal direction, $\mathbf{n}$, lies in the radial direction, $\mathbf{n}=\mathbf{e}_r$. The ϕ coordinate curve corresponding to point P is drawn simply to demonstrate that, for all ϕ, $\mathbf{e}_\phi$ has zero projection onto the z axis: $\mathbf{e}_\phi \cdot \mathbf{e}_z = 0$.

The configuration is stable if (i) the interface between fluids remains flat and (ii) the centers of the particles remain in the interfacial plane. We shall estimate the criteria that should be satisfied by the shear rate for these two conditions to hold.

Equation (15), for the pressure field, shows that a pressure difference $\sim|\eta_1 - \eta_2|\alpha_{ij}$ exists between the fluid in $z>0$ and that in $z<0$, a quantity proportional in magnitude to the shear viscosity contrast. Such a pressure difference must be balanced by the pressure due to curvature in the interface, $\sim\tau/R$ (τ is surface tension). This curvature will be small for shear rates, which satisfy

$$\alpha_{ij} \ll \frac{\tau}{|\eta_1 - \eta_2|R}. \tag{A1}$$

Next we calculate the distribution of force, $\mathbf{F}$, acting over the surface, $r=R$, of the interface-embedded solid particle. In our Cartesian coordinate system of Fig. 1, the components of the stress tensor may be obtained, on $r=R$, by substituting a velocity obtained from Eq. (14) into the definition of the stress, $\sigma_{ij} = -p\delta_{ij} + \eta(\partial_i v_j + \partial_j v_i)$, then setting $r=R$ in the resulting expressions. The resulting surface force, $F_j = \int_{s_1+s_2}[\sigma_{ij}]_{r=R} n_j dA$ (notation of Sec. III) may, straightforwardly, be shown to be

$$F_x = F_y = 0, \quad F_z = 5\pi R^2(\eta_1 - \eta_2)\alpha_{zz}. \tag{A2}$$

There is no resultant force on the sphere in the z or y direction. The component F_z of the force is counterbalanced by the force $F=2\pi\tau q_c$, where $q_c=r_c \sin\psi$ is the "capillary charge" of the particle, $r_c \approx R$ is the radius of the contact line, and ψ is the meniscus slope angle [29]. The value $\psi=0$ corresponds to the flat interface. The requirement $\psi \ll 1$ leads to the same form of the stability criterion as given by Eq. (A1).

Substituting into Eq. (A1) the typical values $\tau \sim 10^{-2}$ J/m^2, $|\eta_1-\eta_2| \sim 10^{-3}$ kg/m s, $R \sim 10^{-5}$ m yields inequality for the shear rate $\alpha_{ij} \ll 10^6$ s^{-1}, which is a rather weak requirement.

APPENDIX B: SIMULATION METHOD

This appendix summarizes the method of Ref. [25] and its adaptation to the present problem. The single-time relaxation LB method, also known as lattice Bhatnagar-Gross-Krook, is defined by the evolution equation for the momentum distribution function f_i [24]:

$$f_i(\mathbf{r}+\mathbf{c}_i, t+1) = f_i(\mathbf{r},t) - \frac{1}{\tau}[f_i(\mathbf{r},t) - f_i^e(\rho,\rho\mathbf{u})]. \tag{B1}$$

f_i represents a population of particles with velocity $\mathbf{c}_i$; the set $\mathbf{c}_i$ defines the lattice. Associated with link i is weight t_p. The values of $\mathbf{c}_i$'s and equilibrium distribution f_i^e for the D3Q15 lattice used here are defined in Ref. [25]. The nodal density, ρ, and the nodal momentum, $\rho\mathbf{u}$, are defined by the moments of f_i with $\mathbf{c}_i$. Parameter τ (BGK relaxation time) determines the lattice fluid's kinematic viscosity $\nu=\frac{1}{6}(2\tau-1)$ [24].

N particles of radius R are inserted at random positions in the plane $z=0$. The particles are allowed to move in this plane and rotate around the normal to the plane. We treat the particle interior as being occupied by a fluid in a state of uniform translation and rotation determined by the motion of the particle boundary. On the particle surface we use a type of no-slip boundary condition given by Ladd [30]:

$$f_{-i}(\mathbf{r}_w, t+1) = f_i(\mathbf{r}_w,t) + \frac{2\rho t_p}{c_s^2}(\mathbf{w}_k \cdot \mathbf{c}_1), \tag{B2}$$

where $\mathbf{w}_k$ is the velocity of the boundary of the kth particle, $c_s=1/\sqrt{3}$ is the speed of sound for D3Q15 model used in this study the weights, t_p, of which are defined in Ref. [25]. Equation (B2) represents the effect of moving particles' boundaries on the embedding fluid and can be used to compute the effect of forces and torques impressed upon the particles by the fluid. Because we investigate the low surface particle concentration, we omit the sublattice lubrication force for particles in close approach, inserted into this algorithm by Nguyen and Ladd [31].

LE boundary conditions [26], after Wagner [27], are applied in this study. For embedded particles migrating across the LE boundary, any portion of the particle surface that has passed the boundary is reintroduced (from the periodic replica) having been displaced and accelerated. For a boundary parallel to the shear direction, $\mathbf{e}_x$, the reentrant portion of a crossing particle is displaced (advected) by the action of the LE velocity $v_{LE}\mathbf{e}_x$ through distance $v_{LE}\mathbf{e}_x\Delta t$ (with the simulation time step $\Delta t=1$) and accelerated by addition of the LE velocity $v_{LE}\mathbf{e}_x$. Wagner's method is applied to all (including interior) fluids at the LE boundary. Update of particle position and velocity on the LE boundary is made after the LB collision step.

To calculate total dissipation using Eq. (31), the appropriate velocity derivatives are evaluated from a discrete approximation nonlocally using the isotropy properties of the D3Q15 lattice:

$$\frac{\partial u_\alpha}{\partial x_\beta} = \frac{1}{c_s^2}\sum_i t_p u_\alpha(\mathbf{r}+\mathbf{c}_i)c_{i\beta} + o(\mathbf{c}_i^3). \tag{B3}$$

Data for a range of particle sizes were obtained on a lattice of size $128\times128\times128$. The fluid was initialized to a uniform density $\rho=1.8$. The value of the relaxation parameter $\tau=1.0$ used corresponds to an optimum of performance in locating the boundary using bounce-back boundary conditions [24]. A number $N=1,\ldots,36$ of particles of radii $R=6,7,8,10$ were considered. LE boundary conditions were imposed by a LE velocity $v_{LE}=0.05$. An effective hydrodynamic radius of the particles was obtained by correction $R\rightarrow R+\Delta R$ with $\Delta R=-0.78$ [25]. In all cases the Reynolds number $\mathrm{Re} \equiv v_{LE}R^2/(L_y\nu)$ did not exceed the value 0.25, which is small enough to signify a linear rheological response.

[1] P. Pieranski, Phys. Rev. Lett. **45**, 569 (1980).
[2] W. Ramsden, Proc. R. Soc. London **72**, 156 (1903).
[3] B. P. Binks and T. S. Horozov, *Colloidal Particles at Liquid Interfaces* (Cambridge University Press, Cambridge, England, 2006).
[4] A. Böker, J. He, T. Emrick, and T. Russel, Soft Matter **3**, 1231 (2007).
[5] A. Menner, R. Verdejo, M. Shaffer, and A. Bismarck, Langmuir **23**, 2398 (2007).
[6] L. Torres, R. Iturbe, M. J. Snowden, B. Chowdhry, and S. Leharne, Chemosphere **71**, 123 (2008).
[7] B. Neirinck, T. Mattheys, A. Braem, J. Fransaer, O. van der Biest, and J. Vleugels, Adv. Eng. Mater. **10**, 246 (2008).
[8] B. Neirinck, J. Fransaer, O. Van der Biest, and J. Vleugels, Adv. Eng. Mater. **9**, 57 (2007).
[9] H. Strohm and P. Löbmann, J. Mater. Chem. **14**, 2667 (2004).
[10] A. D. Dinsmore, M. F. Hsu, M. G. Nikolaides, M. Marquez, A. R. Bausch, and D. A. Weitz, Science **298**, 1006 (2002).
[11] E. Vignati, R. Piazza, and T. P. Lockhart, Langmuir **19**, 6650 (2003).
[12] B. Cichocki, M. L. Ekiel-Jezewska, G. Nagele, and E. Wajnryb, Europhys. Lett. **67**, 383 (2004).

[13] P. Denissenko, G. Falkovich, and S. Lukaschuk, Phys. Rev. Lett. **97**, 244501 (2006).
[14] B. Cichocki, M. L. Ekiel-Jezewska, and E. Wajnryb, J. Chem. Phys. **126**, 184704 (2007).
[15] A. Einstein, Ann. Phys. **324**, 289 (1906).
[16] D. E. Tambe and M. M. Sharma, J. Colloid Interface Sci. **162**, 1 (1994).
[17] M. L. Henle and A. J. Levine, Phys. Fluids **21**, 033106 (2009).
[18] P. G. Saffman and M. Delbrück, Proc. Natl. Acad. Sci. U.S.A. **72**, 3111 (1975).
[19] G. K. Batchelor, *An Introduction to Fluid Dynamics* (Cambridge University Press, Cambridge, England, 2002).
[20] L. D. Landau and E. M. Lifshitz, *Fluid Mechanics* (Pergamon Press, New York, 1987).
[21] R. Aris, *Vectors, Tensors, and the Basic Equations of Fluid Mechanics* (Dover Publications, New York, 1989).
[22] H. J. Wilson and R. H. Davis, J. Fluid Mech. **452**, 425 (2002).
[23] J. F. Brady, A. S. Khair, and M. Swaroop, J. Fluid Mech. **554**, 109 (2006).
[24] S. Succi, *The Lattice Boltzmann Equation for Fluid Dynamics and Beyond* (Oxford University Press, New York, 2001).
[25] S. V. Lishchuk, I. Halliday, and C. M. Care, Phys. Rev. E **74**, 017701 (2006).
[26] A. W. Lees and S. F. Edwards, J. Phys. C **5**, 1921 (1972).
[27] A. J. Wagner and I. Pagonabarraga, J. Stat. Phys. **107**, 521 (2002).
[28] P. Cicuta, E. J. Stancik, and G. G. Fuller, Phys. Rev. Lett. **90**, 236101 (2003).
[29] P. A. Kralchevsky and K. Nagayama, Adv. Colloid Interface Sci. **85**, 145 (2000).
[30] A. J. C. Ladd, J. Fluid Mech. **271**, 285 (1994).
[31] N. Q. Nguyen and A. J. C. Ladd, Phys. Rev. E **69**, 050401(R) (2004).